Molybdenum Silicide Based Materials and Their Properties

Z. Yao, J. Stiglich, and T.S. Sudarshan

(Submitted 16 November 1998; in revised form 4 February 1999)

Molybdenum disilicide ($MoSi_2$) is a promising candidate material for high temperature structural applications. It is a high melting point (2030 °C) material with excellent oxidation resistance and a moderate density (6.24 g/cm^3). However, low toughness at low temperatures and high creep rates at elevated temperatures have hindered its commercialization in structural applications. Much effort has been invested in $MoSi_2$ composites as alternatives to pure molybdenum disilicide for oxidizing and aggressive environments. Molybdenum disilicide-based heating elements have been used extensively in high-temperature furnaces. The low electrical resistance of silicides in combination with high thermal stability, electron-migration resistance, and excellent diffusion-barrier characteristics is important for microelectronic applications. Projected applications of $MoSi_2$-based materials include turbine airfoils, combustion chamber components in oxidizing environments, missile nozzles, molten metal lances, industrial gas burners, diesel engine glow plugs, and materials for glass processing. In this paper, synthesis, fabrication, and properties of the monolithic and composite molybdenum silicides are reviewed.

Keywords molybdenum disilicide, $MoSi_2$, oxidation resistance, tribology

1. Introduction

Advanced gas turbine parts are subjected to increasingly severe mechanical, thermal, and corrosive environments. Prior efforts have resulted in the development of several generations of superalloys. However, these alloys require cooling during engine operation, and practical temperature limits for metallic alloys (including active cooling) are now at <1100 °C, which makes further turbine inlet gas temperature increases prohibitively difficult and expensive. Since 1985 there have been no major breakthroughs in the development of nickel-base superalloys (Ref 1).

The drive toward advanced high thrust-to-weight ratio propulsion systems requires the development of high strength and low-density structural materials capable of extended operation at temperatures as high as 1600 °C. Intermetallics such as nickel and titanium aluminides have been extensively studied and are currently being developed. These intermetallics have the advantage of a lower density than superalloys, but their melting temperatures of 1400 to 1600 °C limit their maximum use temperatures to approximately 1200 °C (Ref 2).

Molybdenum disilicide ($MoSi_2$) is a high melting point (2030 °C) material with excellent oxidation resistance and a moderate density (6.24 g/cm^3), which is in use in high temperature furnaces because it can withstand prolonged exposure in air. It is a promising candidate material for high temperature structural applications, particularly in aircraft gas turbine engines. Molybdenum disilicide-based composites have emerged as important elevated temperature structural materials for applications in oxidizing and aggressive environments (Ref 2-5).

Z. Yao, J. Stiglich, and **T. S. Sudarshan,** Materials Modification, Inc., P-1, Fairfax, VA 22031, USA. Contact e-mail: sudarshan @matmod.com.

Current potential applications of $MoSi_2$-based materials include turbine airfoils, combustion chamber components in oxidizing environments, missile nozzles, molten metal lances, industrial gas burners, diesel engine glow plugs, and materials for glass processing. In microelectronic devices, thin silicide layers are used as contacts and interconnections because they have low electrical resistance, high thermal stability, high electron-migration resistance, and excellent diffusion-barrier characteristics (Ref 6).

Molybdenum disilicide was discovered in 1907 (Ref 7) and was considered a high-temperature, corrosion-protective coating material for ductile metals. The first commercial heating

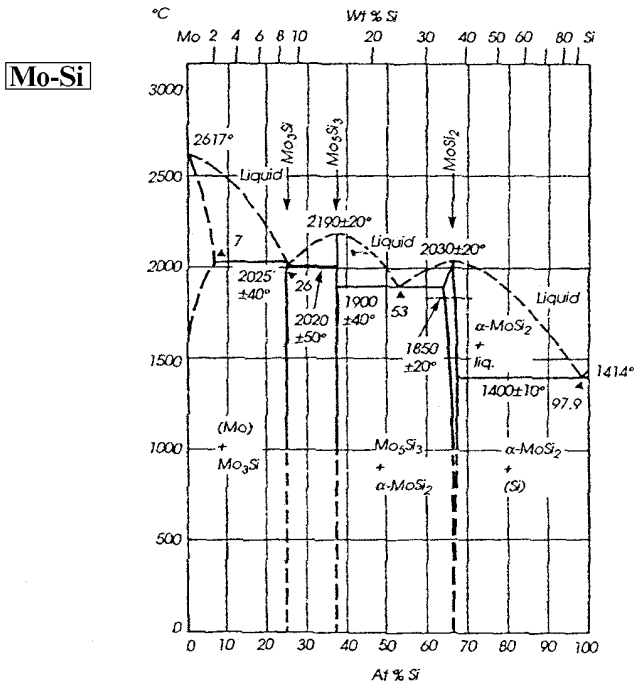

Fig. 1 Binary phase diagram between Mo-Si (Ref 9)

elements were patented by Kanthal in 1953 (Ref 8). Figure 1 shows the binary molybdenum-silicon equilibrium diagram (Ref 9). Three molybdenum-silicon stoichiometries have been found, which are Mo_3Si (cubic), Mo_5Si_3 (tetragonal), and $MoSi_2$ (tetragonal). The crystal structure of $MoSi_2$ is $C11_b$ type, space group $I4/mmm$. The lattice parameters are a = 0.3205 nm and c = 0.7845 nm with c/a = 2.45 (Fig. 2). Molybdenum atoms occupy (0, 0, 0) and (1/2, 1/2, 1/2) positions, and silicon atom positions are (0, 0, 1/3), (0, 0, 2/3), (1/2, 1/2, 1/6), and (1/2, 1/2, 5/6). The unit cell can be thought of as consisting in three squashed cubic pseudocells stacked in the c direction, with each pseudocell containing an atom at its body center.

Until recently, it was believed that $MoSi_2$ exhibited the tetragonal $C11_b$ structure (low temperature α-phase) below 1900 °C and the hexagonal $C40$ structure (high temperature β-phase) between 1900 °C and its melting temperature of 2030 °C. However, recent investigations reveal that the $C11_b$ structure (α-phase) is maintained up to the melting point, and the previously reported high-temperature $C40$ phase (β-phase) is stabilized by impurities (Ref 10).

2. Synthesis of Molybdenum Silicides

Conventionally silicides are processed either by arc melting or siliciding of molybdenum powders. These processes are energy intensive and require long homogenization times in order to obtain desired products. The high melting point of $MoSi_2$ prohibits the conventional melting approach, and the loss of silicon by volatilization during arc melting can result in the formation of undesirable intermediate phases. In addition, the silicide powders obtained by these routes have high oxygen contents and other impurities, which are unacceptable for high-temperature structural applications and for the fabrication of microelectronic devices. Considerable interest and effort are being invested in the development of $MoSi_2$ with low oxygen content (Ref 11).

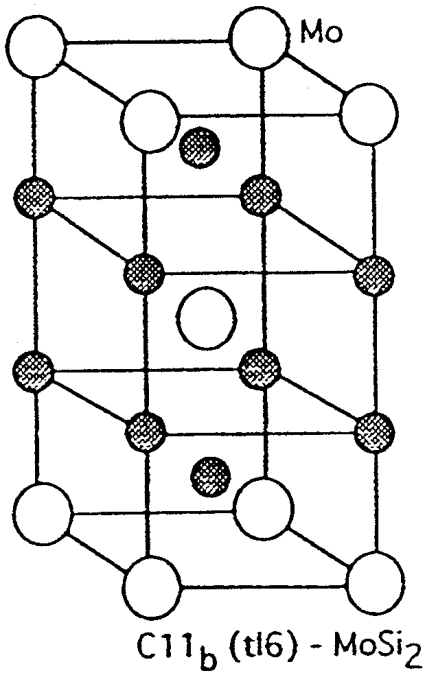

Fig. 2 Crystal structure of $MoSi_2$ (Ref 6)

2.1 Mechanical Alloying

Mechanical alloying is an intensive high-energy milling process and has been used to synthesize $MoSi_2$ from elemental powder blends (Ref 11-17). The process involves repeated fracturing and welding of powders (both metallic and nonmetallic) in a highly energized ball mill. The fracturing of the powders by the grinding media produces clean surfaces, and when these surfaces come in contact they are welded together. The kneading of powders due to repeated fracturing and welding leads to alloying at the atomic level. The oxygen content of $MoSi_2$ powders can be reduced to 310 ppm by weight by using high purity molybdenum and silicon powders and performing mechanical alloying inside an argon-filled glove box (Ref 12).

The formation of $MoSi_2$ and the relevant reaction rate during mechanical alloying of molybdenum-silicon powder mixtures critically depend on the powder composition (Ref 11). The abrupt formation of $MoSi_2$ and the rapid reaction rate at the stoichiometric composition indicate that a mechanically induced self-propagating reaction (MSR) is principally responsible for the $MoSi_2$ formation. The MSR does not occur at the silicon-rich and silicon-poor compositions. Instead, the formation of $MoSi_2$ at the nonstoichiometric compositions is characterized by the gradual formation of both $MoSi_2$ (α-phase and impurities-stabilized $MoSi_2$ (β-phase).

Although mechanical alloying has proven to be versatile in processing amorphous and crystalline silicides, large-scale production of mechanically alloyed materials has not been realized. A significant problem with mechanical alloying is the contamination of the powders/products by gases such as oxygen and nitrogen as well as contamination by the media and the container. These contaminants can form glassy phases and segregate to grain boundaries, resulting in poor mechanical properties. In most systems, mechanical alloying requires ~10 h to achieve equilibrium and stable phases.

High-energy attrition of conventional $MoSi_2$ powder (99.5% purity, –325 mesh, oxygen content: 0.54 wt%) in liquid nitrogen for 30 h has produced nano $MoSi_2$ (22 to 33 nm) powders with a very high oxygen content (4 to 6 wt%) (Ref 18). The oxygen contamination possibly results from the condensation of water vapor from the atmosphere onto the cold milling container and the powder during or after the attrition run. A very high nitrogen content (2 to 3 wt%) has also been observed due to the milling of the powder in liquid nitrogen during the high energy attrition (nitrogen content: 0.01 wt% in the starting $MoSi_2$ powder).

Sonochemical coreduction of $MoCl_5$ and $SiCl_4$ with sodium/potassium (Na/K) alloy in a hexane dispersion, followed by annealing at 900 °C produces nanocrystalline $MoSi_2$ powders (16 to 31 nm) with a 90% yield. However, this process is limited to small quantities (up to 5 g), and large-scale experiments have suffered from the incorporation of minor amounts of the silicon-deficient byproduct phase Mo_5Si_3 (Ref 19). Other efforts have also been made to synthesize nano $MoSi_2$ powders (Ref 20).

2.2 Combustion Synthesis

The large negative enthalpy of formation for $MoSi_2$ allows it to be synthesized by thermal ignition of molybdenum-silicon powdered compacts, a method known as combustion synthesis or self-propagating, high-temperature synthesis (SHS) (Ref 21-27). Combustion synthesis utilizes the exothermic heat of reaction between elements/compounds to synthesize useful intermetallic compounds. Combustion reactions take place either in the self-propagating mode or the thermal explosion mode. A self-propagating reaction occurs when the reaction is initiated locally in the compact and propagates as a wave front through the compact. In the explosion mode, the powder compact is heated in a furnace until combustion occurs simultaneously in the whole compact. Advantages of combustion synthesis include a simple reactor, a very low energy requirement, the ability to simultaneously synthesize and densify the product, tailored microstructures and properties, higher purity of the products, and the synthesis of metastable phases. One disadvantage is the generation of pores and cracks due to the violent nature of the reaction, thermal shock, and steep thermal gradients.

Molybdenum disilicide has been prepared by many research groups using the combustion synthesis route (Ref 21-27). Stoichiometric $MoSi_2$ has been obtained by igniting a compact of stoichiometric elemental mixtures. Compact diameters of 20 mm and greater are needed to ensure a complete conversion of reactants and to obtain single-phase $MoSi_2$. Theoretical calculations of the adiabatic temperature for $MoSi_2$ indicate that this reaction is on the border of being self propagating. To ensure a complete reaction, synthesis of $MoSi_2$ was carried out in the thermal-explosion mode and the chemical-oven approach in addition to the self-propagating mode. Preheating the reactants or using an inert atmosphere results in higher combustion temperatures and combustion velocities. Quenching experiments established the formation of $MoSi_2$ in a single step during combustion synthesis, while differential thermal analysis established two reaction mechanisms for the formation of $MoSi_2$. With lower heating rates (<100 °C/min), a solid-state reaction to form Mo_5Si_3 was followed by a reaction between Mo_5Si_3 and molten silicon to yield $MoSi_2$. At higher heating rates (>100 °C/min), a liquid silicon-solid molybdenum reaction occurred, leading to the formation of $MoSi_2$, which is typical of a combustion reaction.

A field-activated combustion synthesis (FACS) process, combined with the application of mechanical pressure, was used to produce dense $MoSi_2$ from molybdenum and silicon powders (Ref 28). Combustion synthesis was carried out under the combined effect of an electric field and mechanical pressure. The process involved the application of pressure to the reactants under vacuum, the imposition of pulsed electric current, followed by a continuous current until the maximum temperature was reached, and the cooling of the product at a constant rate. No reaction between molybdenum and silicon powders occurred at 1400 °C, but at 1700 °C, $MoSi_2$ formed and densified. Highly dense molybdenum silicide up to (99.2%) was produced from elemental powders in one step. Minor amounts of Mo_5Si_3 were present at the boundaries of $MoSi_2$ grains in the interior of samples made from stoichiometric reactants. The addition of 2.5 mol% Si excess resulted in Mo_5Si_3-free, dense $MoSi_2$ products.

2.3 Shock Synthesis

The application of a high-energy shock wave to induce reactions in a mixture of powders formed the foundation of the shock synthesis process. Shock compression of elemental powder mixtures can lead to chemical reactions resulting in the formation of equilibrium and nonequilibrium compounds. Shock application to powder mixtures results in extensive plastic deformation, fluidlike turbulent flow, particle comminution, and the mixing of constituents having fresh and clean surfaces. In addition, irreversible changes in the starting composition, volumetric distribution of constituents, and shape of the void space were produced as a result of shock compression. Shock processes are best described in terms of departures from equilibrium and can be classified into two types, shock-assisted and shock-induced reactions (Ref 29).

Chemical reactions occurring in shock-modified powder mixtures are termed shock-assisted reactions. Shock-assisted reactions are initiated due to bulk temperature increases that occur on the time scale of thermal equilibrium but at times significantly greater than for pressure equilibrium. Shock-induced reactions are those that are limited to, and occur within, the time scales associated with pressure equilibrium. Shock-induced reactions are difficult to monitor experimentally because they occur with relatively small changes in bulk properties.

Shock synthesis has been used to synthesize molybdenum silicides. Recovery experiments in the molybdenum-silicon system reveal fully reacted, partially reacted, and unreacted regions (Ref 30). Partial reactions are characterized by the presence of large pores/voids, while the unreacted regions are consolidated to near theoretical density. Fully reacted regions are characteristic of a completely reacted, melted, and resolidified material. The extent of a shock-synthesis reaction increases with an increase in shock energy, temperature, and enthalpy of the reaction. Based on electron microscopic observations, a self-sustaining mechanism for the formation of molybdenum silicides has been proposed. The reaction is initiated at the interface between molybdenum and silicon. After initial solidification, the product is spheroidized due to surface tension forces and eventually squeezed out into the interface, thus, exposing a newer surface for the reaction to initiate. As a result, a constant metal-molten silicon interface is maintained at all times.

2.4 Chemical Vapor Deposition

Chemical vapor deposition (CVD) is a process wherein vapor phase reactants form a coating, which is deposited on a heated surface. The process is versatile and can be used to apply coatings to a substrate in order to improve wear resistance, corrosion resistance, strength, and electrical conductivity. The most attractive feature of CVD is its ability to deposit thin films in crevices and deep recesses that are encountered in electronic circuits. Prior to conducting CVD in any system, it is necessary to evaluate various process parameters such as precursor, deposition temperature, substrate temperature, and substrate material with the help of thermodynamic principles. When the

process of CVD is used to infiltrate a porous body, it is called chemical vapor infiltration (CVI).

Chemical vapor deposition and chemical vapor infiltration (CVI) have been used to deposit molybdenum silicides. The source of silicon can be SiH_4, SiH_2Cl_2, $SiHCl_3$, or $SiCl_4$, and the source of molybdenum can be MoF_6 or $MoCl_5$ (Ref 31). The characteristics of the deposited silicide films are influenced by a number of variables. These include substrate temperature, deposition temperature, pressure, and ratio of the precursors. Substrate cleanliness is very important in order to prevent any difficulties during subsequent processing steps such as annealing or contact metallization.

Reactive vapor infiltration (RVI) has also been explored to produce $MoSi_2$ (Ref 32). Molybdenum in the form of a fine porous powder compact is converted to $MoSi_2$ by silicon vapor. In the RVI process, a loosely compacted metallic molybdenum powder is exposed to silicon vapor at temperatures slightly below the melting point of silicon. Silicon vapor can be supplied through a gas-phase decomposition of $SiCl_4$ in the presence of hydrogen gas. The sample cross sections show a thick $MoSi_2$ external layer, a thin Mo_5Si_3 intermediate layer, and an unreacted molybdenum core. These observations suggest that, at the onset of the process, molybdenum reacts with silicon to form Mo_5Si_3 and a further supply of silicon converts Mo_5Si_3 to $MoSi_2$. As the process proceeds, silicon diffuses through the surface $MoSi_2$ layer, successively converting each molybdenum particle to Mo_5Si_3 and then to $MoSi_2$ so that distinct fronts of Mo_5Si_3 and $MoSi_2$ move progressively inward from the surface of the compact.

3. Consolidation of Molybdenum Disilicide

Molybdenum disilicide-based heating elements are produced by powder metallurgy (Ref 33). In the process, the lubricant mixed powder is extruded into straight rods of different diameters for the terminals and heating zones. The rods are dried, sintered, and cut into suitable lengths. The heating zones are bent under heat to the desired shape and welded to the terminals, one end of which is conically ground to the same diameter as that of the heating zone. The other end of the terminal is aluminized to ensure a good electrical contact.

Hot pressing has been used to consolidate $MoSi_2$ specimens (Ref 34-35). The $MoSi_2$ powder was hot pressed for 15 min from 1500 to 1920 °C to achieve a distribution of grain sizes. High density (>97% of the theoretical) and uniform microstructures are obtained. Grain boundaries and secondary phases were clearly visible without etching of the material. Compacts prepared at temperatures from 1500 to 1800 °C contained slight porosity along grain boundaries, independent of grain size, with large pores approximately 10 μm in diameter, while the specimen consolidated at 1920 °C was fully dense. Small amorphous spherical SiO_2 particles, which were independent of grain size, were observed within the $MoSi_2$ grains and at grain boundaries in all specimens, with a median size of 2 μm. Above approximately 1750 °C, volatile SiO(g) and solid Mo_5Si_3 were created from $MoSi_2$ and SiO_2. The increased surface reactivity due to SiO volatilization is a likely mechanism for the observed rapid increase in $MoSi_2$ grain size. Above 1900 °C, a $MoSi_2$-Mo_5Si_3 eutectic liquid was formed. Increased grain size and lack of porosity in the specimen consolidated at 1920 °C were consistent with the effects of liquid-phase sintering. Trace amounts of β-SiC likely resulted from a liquid-phase reaction between liquid silicon and carbon (die materials) at the compact surface.

Hot isostatic pressing (HIP) has also been used to evaluate densification of $MoSi_2$ specimens as a function of temperature, pressure, and time (Ref 36-40). Molybdenum disilicide powders were consolidated by HIP at 207 MPa pressure, in the temperature range of 1200 to 1400 °C for 1 and 4 h. The higher and the longer the temperature and the time, the higher the densities were. A relative density of 99% was observed in a specimen consolidated at 1400 °C for 4 h. Grain sizes in the $MoSi_2$ specimens varied from 23 to 34 μm over the range of process conditions considered. The grain size increase with temperature (ΔT = 200 °C) was of the order of 7 μm and that with time (δt = 3 h) was at most 3 μm. The absence of fine grains in the consolidated specimens suggested that diffusion was probably not the primary densification mechanism. The presence of cusped pores, the observed grain sizes, and the low diffusivities of the constituents suggested that densification was most likely dominated by power law creep (PLC). It was found that slow cooling (<5 °C/min) under full pressure or slowly released pressure (~2 MPa/min) produced the best material. Rapid cooling or rapid release of pressure at elevated temperatures resulted in microcracking in the consolidated material.

Hot isostatic pressing has also been used to consolidate nanocrystalline $MoSi_2$ powders produced by high-energy attrition (Ref 18). It was found that the nanocrystalline $MoSi_2$ powders are easy to process into bulk shapes as compared to large-grained $MoSi_2$ powders. Before HIP, large grained $MoSi_2$ powders must be cold-isostatic pressed at lower pressures to avoid fracture after consolidation.

Plasma spray processing is a promising near-net shape manufacturing technology, combining melting, blending, and consolidation into a single operation (Ref 41). Rapid solidification rate (RSR) processing is an inherent characteristic of plasma spray processing and yields fine-grained and chemically homogeneous microstructures. Low-pressure plasma spraying (LPPS) and vacuum plasma spraying (VPS) are important processing methods for fabrication of RSR-processed deposits. The advantages of VPS processing include dense and oxide-free deposits. During VPS processing, the substrate-deposit system is exposed to high temperatures (800 to 900 °C) due to a reduced rate of heat removal and adiabatic recalescence. This causes annealing of the VPS deposit, leading to stress relief, improved interparticle bonding, and recrystallization, without any significant grain growth.

Vacuum plasma spraying has been used to fabricate dense $MoSi_2$ (Ref 41-42). $MoSi_2$ powder, with an average particle size of –44 μm (–325 mesh) and oxygen content of 2400 ppm has been used to generate deposits with a high hardness, indentation fracture toughness, and flexural strength. It was observed that annealing increased fracture toughness and flexural strength due to improved interparticle bonding. Freestanding forms of $MoSi_2$ were annealed at 1100 °C in flowing argon for 24 h and furnace cooled. In the as-sprayed deposits, RSR processing associated with VPS produced the hexagonal allotrope

of $MoSi_2$ (impurities-stabilized β phase), which transformed to the tetragonal structure upon annealing. Elevated-temperature testing showed that $MoSi_2$ increased ductility, which can be an advantage in forming of these plasma-processed materials.

4. Single Crystal $MoSi_2$

To further evaluate the feasibility of molybdenum disilicide for high temperature applications, basic deformation mechanisms and physical properties need to be determined. These measurements are best conducted on single-crystal samples. However, the preparation of single crystals of $MoSi_2$ is a significant technical challenge (Ref 43-46). Molybdenum disilicide melts at temperatures greater than most standard crucible materials, preventing the application of conventional techniques such as Bridgman or Czochralski methods. The vapor pressure of silicon at the melting point of $MoSi_2$ is 0.1 torr, and stoichiometry during preparation and the growth of crystals must be carefully controlled.

Many techniques such as electron beam float zone, inductively coupled plasma pedestal growth, and induction float zone in atmospheric and pressurized chambers have been explored for the synthesis of single crystals of $MoSi_2$ (Ref 43). One major concern is the high vapor pressure of silicon at the melting point, which can result in silicon loss and the formation of Mo_5Si_3. The degree to which silicon is lost is dependent on the melting conditions (ambient pressure, temperature of the melt, and overall time of melting) and is therefore unique to each melting process. With appropriate additions of excess silicon, the composition can be controlled to yield crystals of stoichiometric $MoSi_2$. The pressurized induction float zone method offers the best potential for compositional control during crystal growth. Some success is demonstrated using induction float zone techniques, but, unfortunately, in order to maintain a stable liquid zone, crystal growth rates three to five times faster than typical float zone growth rates are necessary. As a result, the size of crystals prepared thus far is limited to approximately 3 mm in diameter.

5. Alloys with Other Elements

One attractive feature of $MoSi_2$ is that it can be metallurgically alloyed with other silicides to improve its properties. Table 1 lists various potential high temperature silicides that may be considered for alloying with $MoSi_2$ (Ref 2). Such alloying opportunities make $MoSi_2$ materials more attractive relative to silicon-base ceramics, thus allowing other mechanisms of strengthening to be used in addition to the composite approach.

Tungsten disilicide (WSi_2), which is also tetragonal $C11_b$, forms a complete solid solution with $MoSi_2$ at all compositions. Mechanical alloying has been used to produce Si_2 powders from mixtures of molybdenum, tungsten, and silicon powders in the right proportions. The solid solution was formed in situ by simultaneous mixing of all three constituents (Ref 12). Thermodynamic equilibrium was established when the mechanically alloyed powders were annealed. X-ray diffraction patterns taken from powder heated to 900 °C in a calorimeter show the expected equilibrium phases (Fig. 3). Only one set of Bragg peaks has been observed, which suggests that the annealed equilibrium mixture of $MoSi_2$ and WSi_2 is a solid solution. Another important feature of the mechanical alloying synthesis method is the chemical homogeneity of the alloy. In the $MoSi_2$-WSi_2 alloys, homogeneity is essential for achieving uniform properties. Mixtures of commercial alloy powders of $MoSi_2$ and WSi_2 lack homogeneity (Ref 12). Combination of $MoSi_2$ with disilicides that have the hexagonal C40 structure necessarily require the formation of a two-phase field between the $C11_b$ and C40 phases with various ranges of solubility (Ref 10).

Silicon forms very strong bonds with fluorine, chlorine, and oxygen. Approximate average bond energies are silicon-fluorine, 582 kJ/mol; silicon-chloride, 391 kJ/mol; silicon-oxygen, 336 kJ/mol; and silicon-silicon, 210-250 kJ/mol (Ref 47). However, these energies do not reflect the ease of heterolysis of bonds, which is usual in chemical reactions. In spite of the high silicon-chloride and silicon-fluorine bond energies, compounds containing these bonds are highly reactive. Because charge separation in a bond is a critical factor, the bond ionicities must also be considered when interpreting the reactivities toward nucleophilic reagents. Thus silicon-chloride bonds are much more reactive than silicon-silicon bonds because, though stronger, they are more polar, rendering the silicon more susceptible to attack by a nucleophile such as OH^-. Silica (SiO_2) is relatively unreactive toward Cl_2, H_2, acids, and most metals at ordinary or slightly elevated temperatures, but it is attacked by

Table 1 Potential silicide alloying species for $MoSi_2$ [2]

Silicide	Melting point, °C	Crystal structure	Density, g/cm^3
$MoSi_2$	2030	Tetragonal	6.24
WSi_2	2160	Tetragonal	9.86
$NbSi_2$	1930	Hexagonal	5.66
$TaSi_2$	2200	Hexagonal	9.10
$TiSi_2$	1500	Rhombohedral	4.04

Source: Ref 2

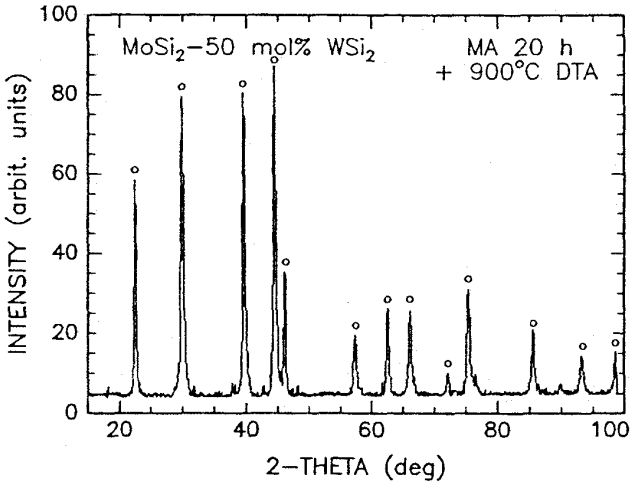

Fig. 3 X-ray diffraction patterns of mechanically alloyed (Mo, W)Si_2 (Ref 12)

fluorine, aqueous HF, alkali hydroxides, fused carbonates, and so on (Ref 47).

Oxygen is invariably incorporated during the synthesis and processing of $MoSi_2$. Oxygen reacts with silicon to form a glassy SiO_2 second phase in the $MoSi_2$ matrix, which is responsible for the excellent oxidation and corrosion resistance of $MoSi_2$. The SiO_2 formed during processing typically segregates to the grain boundaries. The presence of this glassy phase, with a softening temperature close to 1650 °C, is detrimental to the high-temperature strength and creep properties of $MoSi_2$.

Carbon has been added to $MoSi_2$ to reduce oxides (Ref 48-50). Additions of up to 4 wt% C to $MoSi_2$ caused elimination of the siliceous grain boundary phase in hot pressed samples as well as the formation of small quantities of β-SiC and Mo_5Si_3C. Both the hardness and fracture toughness of the carbon-containing alloys exceeded those of the carbon-free (and oxygen-rich) materials. The toughness for all carbon-containing alloys at 800 to 1400 °C was independent of the level of carbon addition, although the hardness at all temperatures up to 1000 °C increased with the level of carbon addition. Unstable fracture was exhibited by all alloys tested below 1200 °C, while stable cracking and high toughness (greater than or equal to 11.5 MPa $m^{1/2}$) was obtained in the 2 wt% C alloy at 1400 °C. However, the large weight losses, which occur during hot pressing are detrimental. It is preferable to deoxidize the $MoSi_2$ chemically prior to hot pressing and then add SiC to the deoxidized powder to form a $MoSi_2$/SiC composite. Leaching reaction-synthesized $MoSi_2$ powder in hot, concentrated sodium hydroxide has been used to remove oxides before hot pressing.

6. Synthesis and Consolidation of Molybdenum Silicide Composites

The use of $MoSi_2$ as a structural material was suggested in the early 1950s because of its excellent oxidation resistance. However, industrial application of $MoSi_2$ has been limited because of the brittle nature of the material at ambient temperatures, a high creep rate at temperatures above 1200 °C, and accelerated oxidation at temperatures between 400 and 500 °C. It was recognized in 1978 that $MoSi_2$ was an important matrix material for high temperature structural composites (Ref 51). Both refractory and ceramic reinforcements have been used in $MoSi_2$ composites. It was reported in 1985 that niobium wire reinforcement significantly improved the room temperature mechanical properties of the $MoSi_2$-Nb composite (Ref 52). Great improvement in room temperature strength and fracture toughness in SiC whisker-$MoSi_2$ matrix composites was demonstrated in 1985 (Ref 53). In 1988 it was established that submicron SiC whisker-$MoSi_2$ matrix composites exhibited mechanical property levels within the range of high temperature engineering applications (Ref 54). In 1990, Los Alamos National Laboratory won a Research and Development 100 Award for its development of $MoSi_2$-SiC composites (Ref 2).

It has been known that fracture toughness of brittle matrices can be improved by the incorporation of a ductile second phase. A key advantage in the use of refractory metal fibers is that they can provide both high-temperature creep resistance and toughness. The ductility of many refractory metal alloys coupled with very high yield and tensile strengths gives their fibers a large fracture energy and the potential to greatly increase the damage tolerance of a brittle matrix composite. Niobium is a suitable ductile reinforcement for $MoSi_2$ because of its high melting temperature and a thermal expansion coefficient, which is close to that of $MoSi_2$. The result will be much less matrix cracking upon thermal cycling during processing and in service (Ref 55-58). Studies have demonstrated that such a composite system indeed exhibits a substantial increase in toughness compared to the matrix alone. Refractory metals such as tungsten, molybdenum, and tantalum have been used as ductile reinforcements (Ref 59).

Several techniques have been used to fabricate $MoSi_2$-Nb composites utilizing niobium in the form of particles, random chopped fibers, and aligned continuous fibers (Ref 55-58). Continuous niobium filaments are necessary to produce significant toughening at room temperature. However, a major problem in using such a composite system is the reaction between the matrix and ductile reinforcement at high temperatures, which leads to formation of brittle interfacial products such as $(Mo,Nb)_5Si_3$. The formation of such interfacial compounds on continuous ductile phases degrades toughness. Therefore, using an inert diffusion barrier coating on the reinforcement prior to processing of composites is essential to reduce interfacial reactions during processing, as well as to maintain the integrity of the reinforcement at elevated temperatures.

Although several attempts have been made to apply inert diffusion barrier coatings in $MoSi_2$/Nb composites, none have succeeded in completely eliminating the formation of interfacial reaction products. Alumina coatings on the surface of niobium have been extensively studied to minimize interfacial reactions between $MoSi_2$ and niobium at high temperatures. Al_2O_3 is chemically compatible with $MoSi_2$ up to 1700 °C and with niobium up to 1500 °C. It also has a thermal expansion coefficient close to those of both $MoSi_2$ and niobium, thus reducing the potential of interfacial crack initiation upon thermal cycling during processing and in service. Several techniques have been used to coat alumina on niobium, including sol-gel coating, physical vapor deposition, and hot dipping in molten aluminum followed by anodizing to form Al_2O_3. Physical vapor deposition produces a dense coating and is the most effective diffusion barrier process for $MoSi_2$/Nb composites. Coatings formed by hot dipping and anodizing are the most porous, while the sol gel derived coatings are cracked. The presence of SiO_2 in the $MoSi_2$ matrix can contribute to dissolution of thin Al_2O_3 coatings and is a significant source of silicon to react with the niobium reinforcement. Thus, improvements in matrix chemistry should be pursued to improve composite performance. Other coatings, such as ZrO_2 and Y_2O_3 have been studied.

Additions of aluminum to $MoSi_2$ have also been studied (Ref 60-61). Aluminum not only modifies the oxide phase present as a coating on the $MoSi_2$ with the reaction $SiO_2 + Al \rightarrow Al_2O_3 + Si$, but also significantly alters the matrix. Aluminum has been reactively infiltrated into $MoSi_2$ preforms with either 40 or 80% density. The resultant fully dense specimens contained $Mo(Al,Si)_2$ particles surrounded by aluminum metal.

One important attribute of $MoSi_2$ is that many potential ceramic reinforcements such as SiC, Si_3N_4, Al_2O_3, Y_2O_3, TiC, TiB_2, and ZrB_2 are thermodynamically stable with $MoSi_2$ (Ref 2). This reinforcement compatibility becomes important for creep and oxidation resistance of these materials. Composites can exist in a $MoSi_2$ matrix reinforced with a ceramic or a ceramic matrix reinforced with $MoSi_2$. It has been shown that the addition of a ceramic phase to $MoSi_2$ substantially improves the elevated temperature strength, creep resistance, and room temperature fracture toughness of monolithic $MoSi_2$.

Silicon carbide reinforced $MoSi_2$ shows improved low-temperature fracture toughness and high-temperature strength (Ref 62-72). The creep properties of $MoSi_2$ have also been successfully enhanced by the addition of SiC whiskers and particles. Although creep mechanisms in $MoSi_2$ composites are not clearly understood, the overall process is possibly due to the combined effects of grain boundary sliding and dislocation glide/climb at high applied stresses, while grain boundary sliding dominates at lower stresses. The chemical species SiC and $MoSi_2$ are thermodynamically stable, hence composites based on these materials have excellent microstructural stability. Composites of $MoSi_2$ with various fractions of SiC particles (up to 40 vol%) have been fabricated from powders by vibratory milling of the powders, followed by hot pressing. It is concluded that the fracture resistance of SiC-$MoSi_2$ matrix composites is primarily governed by the volume fraction of SiC particles. It is observed that optimum toughness can be reached in this material at a volume fraction of approximately 20% SiC. Matrix cracking has occurred during consolidation of an SCS-6 fiber-reinforced composite with the matrix containing up to 40 vol% SiC to modify thermal expansion. Smaller volume fractions of fiber or smaller diameter fibers will be required to minimize matrix cracking. The SiC-C coating applied to SCS-6 fibers has been found to survive consolidation and provide limited debonding in the matrix.

$MoSi_2$/SiC composites have been fabricated by many processing techniques including powder metallurgy, SHS, solid state displacement reactions, exothermic dispersion (XD), and spray forming methods (Ref 62-71). In situ synthesis by solid-state displacement reactions or reactive plasma spraying has been the focus of recent investigations. These techniques appear very promising to produce a homogeneous distribution of the reinforcement phase throughout the $MoSi_2$ matrix and to minimize SiO_2 at grain boundaries, which can lead to improved mechanical properties (Ref 62-73). Reactive plasma spraying to incorporate greater amounts of SiC and/or carbon particulates into $MoSi_2$ by utilizing a higher reactive gas (100% CH_4) has been studied. Low pressure plasma deposition (LPPD) of $MoSi_2$ using 100% methane as a reactive powder carrier has yielded a material with ~6 vol% SiC, ~6% SiO_2, and 13% Mo_5Si_3 and Mo_5Si_3C (Ref 72).

The XD process, in which ceramic particles are formed in situ in molten metal and intermetallic systems, has also been used to fabricate $MoSi_2$ composites (Ref 73-77). Because they are precipitated in situ, the reinforcements are typically single crystals of high purity with clean unoxidized interfaces. The composite materials are crushed into powder and consolidated by sintering. Particulate reinforced $MoSi_2$ composites with 15 to 45 vol% SiC, TiB_2, ZrB_2, and HfB_2, having average particle diameters ranging from 1 to 5 μm, have been produced by the XD process (Ref 76).

Displacement reactions are solid-state diffusional reactions between elements and/or compounds to yield thermodynamically stable phases compared to the starting reactants. Displacement reactions have been applied to the processing of $MoSi_2$/SiC composites (Ref 78). Corresponding diffusion couples were homogenized to yield composites in accordance with the following reaction: $Mo_2C + 5Si \rightarrow 2MoSi_2 + SiC$. Reaction zones in both diffusion couples exhibit an interwoven morphology and contain a homogenous distribution of SiC particulates with an average size of 1 μm in a matrix of $MoSi_2$. The composite was fabricated by hot pressing powder compacts of Mo_2C and Si at 1300 °C for 2 h followed by 1700 °C for 1 h (Ref 21). The final composition in the hot-pressed samples lies in the three-phase field, constituting $MoSi_2$-SiC-Mo_5Si_3C. The reaction characteristics and reaction mechanisms in the formation of $MoSi_2$/SiC composites establish silicon as the fastest diffusing species. The ternary phase (Mo_5Si_3C) is the first to form, followed by the $MoSi_2$ phase. The SiC phase forms at the interface between the ternary phase and $MoSi_2$ and grows into the ternary phase. Although displacement reactions have the ability to produce tailored compositions and microstructures, longer times are needed to homogenize the desired product phases.

The thermal expansion of a fiber and composite matrix should be closely matched in order to minimize thermal stress that develops in a composite due to thermal expansion mismatch. The thermal expansion of Al_2O_3 was close to that of $MoSi_2$, which means that Al_2O_3 fiber is the best selection (Ref 58-59, 78). Modification of the matrix thermal expansion is not required due to the good thermal expansion match between Al_2O_3 and $MoSi_2$. No cracks were observed in the composite matrix during processing or repeated cycling from 1400 °C to room temperature. The use of Al_2O_3 whiskers has been shown to be very effective in improving mechanical properties. $MoSi_2$ composites containing a dispersion of single-crystal Al_2O_3 whiskers and consolidated by extrusion have shown a substantial improvement in flexure strength at temperatures up to 1527 °C. The absence of SiO_2 can be attributed to reduction by carbon that originated in the organic binder used to fabricate the composite. Al_2O_3 fiber bonds strongly to $MoSi_2$, and a proper debond coating is required.

Several techniques have been used to fabricate $MoSi_2$-Al_2O_3 composites, including injection molding of $MoSi_2$-Al_2O_3 aligned short fiber composites, hot isostatic pressing, and plasma spraying of $MoSi_2$-Al_2O_3 lamellar composites (Ref 58-59). Injection molding for fiber alignment consists of four basic steps: feedstock production, fiber alignment, debonding, and consolidation. Feedstock preparation consisted of mixing the powders and fibers with a polymer binder. Fiber alignment comprised injection of the feedstock through a nozzle. Injection was performed above the softening point of the polymer binder. The binder was then removed, either thermally or chemically. Final consolidation was accomplished by sintering or pressure-aided sintering techniques. Dual injection ports allowed spraying of two different powder types, Al_2O_3 and $MoSi_2$. Composites were formed by sequential deposition of $MoSi_2$ and Al_2O_3.

The $MoSi_2$-Si_3N_4 composite system is very interesting and important (Ref 79-82). Additions of Si_3N_4 to a $MoSi_2$ matrix significantly improve the intermediate temperature oxidation resistance of $MoSi_2$ and its elevated temperature mechanical properties. Additions of $MoSi_2$ to a Si_3N_4 matrix allow for the electrodischarge machining of Si_3N_4, and also lead to improved fracture toughness and elevated temperature oxidation characteristics. The addition of ZrO_2 particles to a $MoSi_2$ matrix can produce significant transformation toughening effects in $MoSi_2$ composites (Ref 83). Continuously graded $MoSi_2$-ZrO_2 materials with high density have been fabricated by uniaxial wet molding, followed by hot pressing and hot isostatic pressing. Hot pressed $MoSi_2$-based composites containing Mo_5Si_3, SiO_2, CaO, and TiC as reinforcing second phases have also been investigated in the temperature regime from 1000 to 1300 °C (Ref 84). Fabrication of $MoSi_2$ and α-SiAlON or β′-$SiAlO_n$ composites has also been explored (Ref 85-86).

7. Physical Properties

The properties of $MoSi_2$ make it interesting as a high temperature structural material (Ref 2-5). $MoSi_2$ has a high melting point of 2030 °C and superb high temperature oxidation resistance because it forms a thin coherent, adherent, and protective silica layer. In polycrystalline form, $MoSi_2$ exhibits a brittle-to-ductile transition in compression in the vicinity of 1000 °C. In some orientations of $MoSi_2$ single crystals macroscopic ductility is apparent at much lower temperatures. The material is thermodynamically stable with a wide range of structural ceramics, including Si_3N_4, SiC, Al_2O_3, ZrO_2, mullite, TiB_2, and TiC. There is a significant potential for composite development. It can also be alloyed with other high melting point silicides such as WSi_2 and $NbSi_2$. Due to the metallic nature of its bonding, $MoSi_2$ can be electrodischarge machined, thus making it easier to machine than most structural ceramics. Finally, $MoSi_2$ is an abundant, relatively low cost material, which is also environmentally benign.

In terms of engineering properties, $MoSi_2$ has thermal conductivity between that of Si_3N_4 and SiC. High thermal conductivity is very beneficial for increased cooling effectiveness of engine components. The elastic modulus of $MoSi_2$ is close to that of SiC. While the high temperature oxidation resistance of $MoSi_2$ is similar to that of SiC, maximum oxidation rates in $MoSi_2$ actually occur at a temperature of 500 °C. $MoSi_2$ has a thermal expansion coefficient close to that of Al_2O_3, which is beneficial for minimizing thermal stresses and improving thermal shock resistance. Thermal expansion is also important when designing a composite system. Matching thermal expansion coefficients of matrix and reinforcement is important to minimize the effects of interfacial cracks on subsequent mechanical properties.

The fracture toughness behavior in both $MoSi_2$ and silicon-base ceramics is similar. They both fracture in a brittle manner resulting in low toughness. The toughness levels of monolithic $MoSi_2$ and silicon-base ceramics are in the same range. Thus, it is possible to utilize classical ceramic composite approaches to toughen $MoSi_2$ composites. Commonly, ceramics are reinforced with other ceramic fibers (continuous and discontinuous), whiskers, or particles, with weaker interfacial bonds to permit crack bridging or deflection processes as dominant toughening mechanisms. Other techniques involve phase transformation toughening and elongated grain structures. In each case, the effects are moderate.

In the case of high temperature creep mechanisms, these two classes of materials differ significantly. While silicon-base ceramics exhibit grain boundary sliding and cavitation creep (at low- and high-applied stresses), $MoSi_2$ deforms via matrix dislocation glide and climb (at high stresses), and grain boundary sliding (at low stresses). Both continuous and discontinuous fibers have been used in ceramic materials to improve creep properties. Here it is important that the fiber-matrix interface be strong to impart the load transfer that is necessary to improve creep resistance. Also, elongated grain structures are shown to have beneficial effects by making it difficult for grain-over-grain sliding to occur. Finally, because grain boundary silica contributes to high temperature creep deformation in ceramics, there have been attempts to modify the grain boundary silica phase by additions such as Al_2O_3 and Y_2O_3. This is, however, a difficult approach because the same silica phase is necessary for densification of these ceramics.

7.1 "Pest" Oxidation

One major obstacle for $MoSi_2$ applications is structural disintegration during low temperature oxidation, which is known as the "pest" effect (Ref 87-92). $MoSi_2$ disintegrates to a powder when subjected to oxidizing environments at 400 to 600 °C. This phenomenon was discovered in 1955 and has been referred to as $MoSi_2$ pesting. It has been suggested that the cause is grain boundary embrittlement produced by short-circuit diffusion of O_2 and subsequent dissolution into the grain-boundary areas. However, the exact nature of the pest effect is not clearly understood.

There are two possible oxidation reactions for $MoSi_2$:

$$2MoSi_2\,(s) + 7O_2 \rightarrow 2MoO_3\,(s) + SiO_2\,(s) \quad (1)$$

$$5MoSi_2\,(s) + 7O_2 \rightarrow Mo_5Si_3\,(s) + 7SiO_2\,(s) \quad (2)$$

Both reactions are thermodynamically feasible, but reaction 1 is favored, which results in pesting between 400 and 600 °C. Recent studies on poly- and single-crystalline $MoSi_2$ have shown that the pesting of $MoSi_2$ is associated with a substantial volume expansion, and the disintegrated powdery product contains mainly crystalline MoO_3 whiskers (or platelets), amorphous SiO_2 clusters, and residual $MoSi_2$ crystals. The pest reaction apparently has nucleation and growth stages.

The pest reaction in single-crystalline $MoSi_2$ occurs at a much slower rate than in polycrystalline counterparts (Ref 87). There is no noticeable change in the surface morphology on single crystals oxidized at 500 °C for a few hours. After longer periods (~50 h) of oxidation, the sample surfaces begin to show signs of pesting. The reaction has been found to be highly heterogeneous, only occurring at local areas. The reaction is characterized by the formation of erupted blisters, which exhibit different morphologies on different surfaces and are found to

have compositions similar to Si-Mo-O. Further oxidation of the single crystals has not resulted in blisters but does produce MoO_3 whiskers and SiO_2 clusters. This suggests that blisters may represent an early transient state, and that the Si-Mo-O surface oxide is metastable, evolving further into the thermodynamically stable products MoO_3 and SiO_2 after prolonged oxidation. Disintegration of the $MoSi_2$ single crystals occurs only after prolonged oxidation (>1000 h). Volume diffusion of oxygen is the predominant process in single-crystal $MoSi_2$. Figure 4 presents schematic drawings illustrating the evolution of reaction products during various stages of volume diffusion (Ref 87). Volume diffusion of oxygen gives rise to the formation of a Si-Mo-O surface oxide, erupted blisters, and eventually loosely bound MoO_3 and SiO_2, which in turn causes massive oxidation and surface recession of the sample.

Polycrystalline $MoSi_2$ is much more susceptible to pest disintegration at 500 °C. Both hot-pressed and arc-melted polycrystalline samples have disintegrated into powdery products within a short period of time (10 to 30 h). Pesting also involves grain boundary diffusion of oxygen. Grain boundary diffusion of oxygen causes preferential oxidation of intergranular interfaces and the formation of protruding MoO_3 whiskers. These would result in the formation of internal tensile stresses, which destroy intergranular cohesion.

Experimental results have indicated that $MoSi_2$/AlN and $MoSi_2/Al_2O_3$ composites also exhibit pest disintegration after oxidation at 500 °C. The time required for complete disintegration of $MoSi_2$-Al_2O_3 is much longer (140 h) than that (20 h) for the $MoSi_2$-AlN, suggesting that the reinforcement can affect the kinetics of pesting.

7.2 High Temperature Oxidation

No pesting has been observed in $MoSi_2$ during oxidation above 600 °C. Reaction 2, which does not produce volatile MoO_3, appears dominant. Both static and cyclic oxidation characteristics of $MoSi_2$ materials have been studied (Ref 93-96). Isothermal oxidation experiments have been conducted on specimens exposed in air for 24 h at 800 to 1500 °C. $MoSi_2$ composites have significant isothermal oxidation resistance relative to intermetallic compounds based on titanium, niobium, and tantalum XD composites and the single-crystal, nickel-base superalloy (Ref 2). The protective silica layers are excellent barriers to oxidation attack because of low oxygen permeation rates. $MoSi_2$ is known to exhibit excellent high temperature oxidation behavior up to 1600 °C.

7.3 Strength and Ductility

The major problem impeding use of $MoSi_2$ is its mechanical properties. Because its brittle-ductile-transition temperature (BDTT) is around 1000 °C, its low temperature strength (below 1000 °C) is limited by brittle fracture, while high temperature (above 1000 °C) strength is governed by plastic flow. In this respect and because of its mixed covalent-metallic atomic bonding, $MoSi_2$ is a borderline intermetallic compound. For its effective use as a high temperature structural material, it becomes necessary to toughen the material at lower temperatures (below 1000 °C) while simultaneously improving the strength at higher temperatures (above 1000 °C). Studies on single crystals have shown that as-grown crystals have a low dislocation density with ⟨331⟩ dislocations being found in crystals with a low growth rate and ⟨100⟩ dislocations in crystals with a high growth rate (Ref 97-98).

The ultimate yield stress of the $MoSi_2$-based composites will be higher than the composite yield stress (Ref 2). $MoSi_2$-based composite ultimate yield stress values will have to be determined by tensile testing because of the plasticity that occurs at elevated temperatures. $MoSi_2$-based composite yield stress values are comparable with or exceed structural ceramic ultimate stress values at 1200 °C. At 1500 °C, structural ceramic ultimate yield stress levels are higher than the present $MoSi_2$-based composite yield stress levels. However, a structural ceramic cannot be used at its ultimate yield stress because it will have a 100% probability of catastrophic fracture. Because $MoSi_2$-based composites are at present in their infancy, it is very likely that, with future materials development, the $MoSi_2$-based composite yield stress levels at 1500 °C can be increased by a factor of 2 and perhaps more.

$MoSi_2$-based composites exhibit significant ductility above the $MoSi_2$ BDTT (900 to 1000 °C). The ductility of $MoSi_2$-based composites is at least an order of magnitude greater than

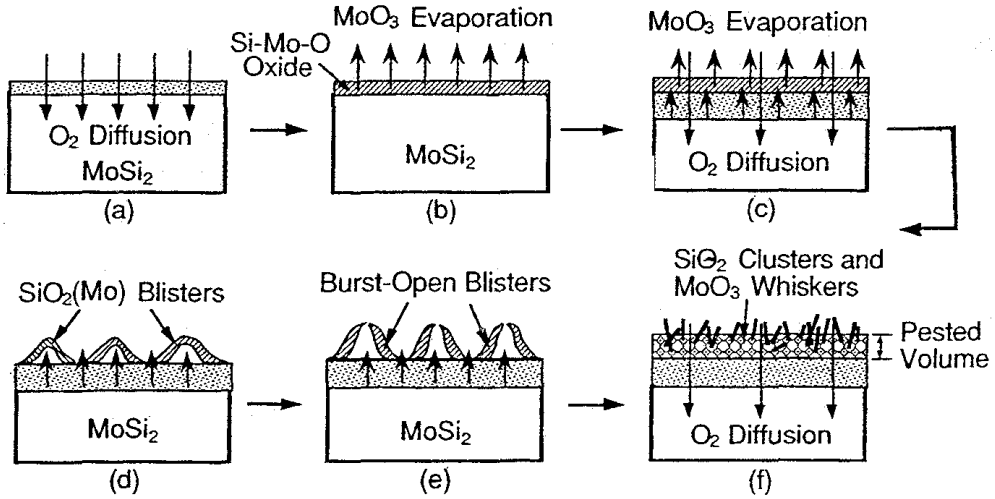

Fig. 4 Schematic drawings of the pesting reaction in a single crystal $MoSi_2$ (Ref 87)

that of the structural ceramics at high temperatures. This ductility means that $MoSi_2$-based composites will have much higher fracture toughness and resistance to catastrophic fracture at elevated temperatures than the structural ceramics. Thus, components made from $MoSi_2$-based composites will be more reliable than components made from structural ceramics.

Studies on single-crystal deformation of $MoSi_2$ and WSi_2 indicate that the strength of these single crystals (although anisotropic) is very good at elevated temperatures (1000 to 1500 °C) (Ref 99-100). The $MoSi_2$ strength at orientations near [001] is significantly higher than for other orientations studied. Such an observation suggests that significant strength improvements (and probably toughness) of polycrystalline silicides could be attained by crystallographic texture control via hot working deformation processing. A 2 wt% C addition to $MoSi_2$, which removes the silica grain boundary phase on $MoSi_2$ particles, improves the Vickers hardness (100 gf load) of the base material (Ref 101). In addition, carbon interacts with $MoSi_2$ to form SiC. Microhardness data at room temperature and at 1000 °C for the carbon-containing alloy shows marked improvement over carbon-free $MoSi_2$.

7.4 Fracture Toughness

The addition of 2 wt% C improves the fracture toughness of $MoSi_2$ dramatically between 800 and 1400 °C, while the fracture toughness of the carbon-free $MoSi_2$ decreases with increasing temperature (Ref 101). The fracture mode has changed from intergranular (no carbon) to transgranular (with carbon) because of removal of a silica grain boundary phase by reaction with carbon. In impure $MoSi_2$ (without carbon), the viscosity of the grain boundary silica decreases with increasing temperature, resulting in grain boundary sliding with cavitation, thereby decreasing toughness. On the contrary, the addition of 2% carbon reduces the grain boundary sliding and improves high temperature toughness because of dislocation motion plasticity.

Generally, a second-phase reinforcement (either brittle or ductile) to $MoSi_2$ has been tried to improve its mechanical properties. Such reinforcement has resulted in two effects, namely improvement of room temperature fracture toughness and improvement of high temperature strength and creep properties, without degrading oxidation resistance.

This improvement has been attributed to crack-deflection-crack branching processes or to the residual stresses at the particle-matrix interfaces. In the XD processed composites, SiC is refined to approximately 2 to 3 μm, giving rise to larger increments in toughness at approximately 20 vol% SiC. On further increasing the SiC volume fraction, the toughness decreased. In this case, it has been observed that the SiC particles fracture. At volume fraction levels greater than 20%, the fractured SiC particles have formed a continuous path, thereby lowering the fracture toughness. On the contrary, TiB_2 reinforcements by the same XD process seem to lower toughness because the TiB_2 particles are pulled out due to weak particle-matrix interfaces. Interestingly, addition of 20 vol% SiC platelets shows the same amount of toughening as SiC particles (Ref 102).

In contrast, $MoSi_2$-ZrO_2 particulate composites exhibit a monotonic increase in fracture toughness with increasing volume fraction of the ZrO_2 reinforcement (Ref 103). These composites contain particles of partially stabilized ZrO_2, which has a metastable tetragonal crystal structure. In the vicinity of the crack tip stress field, the tetragonal particles transform to the monoclinic crystal structure with an associated volume increase of approximately 4%. This crack-induced phase transformation thus produces compressive microstructural stresses, which shield the crack tip from applied external tensile stresses, leading to increased transformation toughening in the composite.

There are limited fracture toughness data on ductile reinforcements. These refractory reinforcements always result in strong matrix-particle interfacial reactions. It is clear that ductile phase reinforcements can result in fairly large improvements in the toughness properties of silicide intermetallics at low temperatures but with a penalty in strength and density, together with high temperature environmental degradation.

7.5 Creep Deformation

Monolithic $MoSi_2$ deforms rapidly at 1200 °C, with creep rates two orders of magnitude higher than SiC whisker-reinforced composite materials (Ref 104-107). The presence of SiC significantly reduces creep rates in the composite. The apparent activation energies are 430 kJ mol^{-1} and 590 kJ mol^{-1} for monolithic and composite $MoSi_2$, respectively. The latter compares well with similar activation energies in Si_3N_4 composites. These activation energies are higher than lattice diffusion energies of silicon in $MoSi_2$. Although such high apparent activation energies have been observed in other materials such as metal matrix composites and dispersion-strengthened alloys, mechanistic understanding is still unclear. In the present case, the overall creep process can be due to the combined effects of grain boundary sliding and dislocation glide and climb mechanisms at higher applied stresses, while grain boundary sliding processes can be dominant at lower stresses.

8. Applications

$MoSi_2$-based materials have been applied in some interesting industrial applications. These applications are driven by the elevated temperature mechanical properties of these materials, in combination with other properties such as electrical conductivity and oxidation/corrosion resistance (Ref 3).

8.1 Heating Elements

$MoSi_2$ materials have been employed for a long time as heating elements for air furnaces. The recent Kanthal (Kanthal AB, Hallstahammar, Sweden) Super 1900 heating elements can operate at an element temperature of 1900 °C in air and oxidizing environments. These Super 1900 elements are actually a solid solution alloy of $MoSi_2$ and WSi_2. The major problems with $MoSi_2$-based heating elements are brittle fracture, which makes the elements difficult to handle, and high temperature creep, which causes the elements to deform and limits their upper use temperature. Both of these aspects limit element life, as well as affect furnace design. Current elements are u-shaped and typically hung vertically due to limitations in mechanical properties. As both the fracture toughness and creep resistance

of $MoSi_2$-based materials continue to improve by composite and alloying approaches, there will be significant improvement in furnace element lifetime as well as greater flexibility in furnace design.

8.2 Aerospace Gas Turbine Engines

Pratt & Whitney has been developing advanced materials for a blade outer air seal (BOAS) hot section component of its gas turbine engines (Ref 3). In the engine, the BOAS is a stationary part, which is located directly opposite the rotating hot section turbine blades. The purpose of the BOAS is to maintain a small gap of stable dimensions between itself and the turbine blade. If this gap widens during operation of the turbine, it directly affects the turbine efficiency. Although stationary, the BOAS is exposed to high turbine gas temperatures and significant thermal stresses.

Gas burner testing by Pratt & Whitney has shown that $MoSi_2$-SiC and $MoSi_2$-Si_3N_4 composites possess significant thermal shock resistance in a simulated jet fuel combustion environment. These materials have survived 250 cycles from room temperature to 1500 °C with no failure. Recent work at NASA Lewis Research Center (Cleveland, OH) has concentrated on $MoSi_2$-Si_3N_4 composites reinforced with SiC continuous fibers. Thermomechanical Charpy impact tests have demonstrated that these composite materials absorb significant impact energy at both room temperature and elevated temperatures.

8.3 Diesel Engines

The Toyota Central Research and Development Facility in Japan has recently developed $MoSi_2$-Si_3N_4 composite diesel engine glow plugs (Ref 3). The $MoSi_2$-Si_3N_4 glow plugs contain 30 to 40 vol% $MoSi_2$ phase in a Si_3N_4 matrix. These glow plugs have two distinct practical advantages over metal glow plugs. First they are highly resistant to the diesel fuel combustion environment and thus have a long lifetime of approximately 13 years. Second, they can be heated at higher heating rates with the result that the diesel engine can be started faster. An inner composite cylinder with an interconnected $MoSi_2$ phase provides the necessary electrical conductivity. An outer, nonconducting sheath of the same $MoSi_2$-Si_3N_4 phase composition is employed as a cover for the inner conducting composite and has the same thermal expansion coefficient and thermal conductivity. This microstructural tailoring of the $MoSi_2$-Si_3N_4 composite allows for optimum performance of the diesel glow plug.

8.4 Industrial Gas Burners

The gas burner industry is in the process of developing burners for oxygen-natural gas mixtures rather than air-natural gas mixtures in order to reduce NO_x environmental emissions (Ref 108). Because such oxygen-natural gas burners must operate at higher temperatures than air-natural gas burners, there is a need to develop new materials that are resistant to the oxygen-natural gas combustion environment. Studies have shown that $MoSi_2$ has significant resistance to oxygen-natural gas combustion at high temperatures. After an initial transient period, material stability is achieved through the formation of a stable Mo_5Si_3 layer. Stability occurs under both stoichiometric and fuel-rich combustion conditions. Prototype $MoSi_2$ gas burners have been fabricated by a plasma spray forming process (Ref 109).

8.5 Molten Metal Lances

Some foundry operations require that gases be injected into molten metals. Microlaminate $MoSi_2$-Al_2O_3 composite tubes have been fabricated by plasma spray forming (Ref 110). These tubes have been tested as inert gas lances in molten aluminum alloys at 725 °C and in molten copper at 1200 °C. The $MoSi_2$-Al_2O_3 composites perform very well in both molten metals. The $MoSi_2$-Al_2O_3 microlaminate tube can withstand at least 4 h in the molten copper, while a graphite tube has lasted for 15 min, and a SiC tube has thermal shocked upon immersion in the molten copper. The $MoSi_2$-Al_2O_3 composite tube is resistant to chemical attack by the molten copper due to the presence of the Al_2O_3 phase, while it exhibits thermal shock resistance and "graceful failure" mechanical behavior due to plastic deformation of the $MoSi_2$ phase.

8.6 Glass Processing

At the present time, metals and ceramic refractories are primarily employed in applications and components requiring contact with molten glasses. Molybdenum is highly resistant to corrosion when immersed in molten glass. However, due to its poor oxidation resistance, it cannot be employed at or above the molten glass line. The precious metal platinum is also employed in contact with molten glasses, but this material is very expensive. The alumina-zirconia-silica (AZS) multiphase refractory ceramic is also used for containing molten glasses but suffers from relatively poor mechanical properties.

Recently, it has been shown that $MoSi_2$ is a material that is quite resistant to corrosion by molten glasses (Ref 111-113). $MoSi_2$ shows excellent corrosion resistance below the glass line due to Mo_5Si_3 formation and excellent oxidation resistance above the glass line due to SiO_2 formation. While corrosion rates of $MoSi_2$ are somewhat higher at the glass line than below the glass line, it has been reported that anodic protection of the $MoSi_2$ significantly lowers corrosion rates at the glass line. This corrosion resistance of $MoSi_2$ to molten glasses in combination with its elevated temperature mechanical properties has recently led the Kanthal Corporation to market a new $MoSi_2$ immersion tube for the injection of gases into molten glass. A CRADA (Cooperative Research and Development Agreement) between the Los Alamos National Laboratory and Schuller International Inc. has been initiated. (Schuller International is a major U.S. producer of fiberglass.) The objective of the CRADA is the development of $MoSi_2$-based materials for fiberglass processing applications and components (Ref 3).

9. Other Efforts

Although $MoSi_2$ has excellent oxidation resistance at temperatures in excess of 1600 °C in air, it has a high creep rate above 1200 °C, making it unsuitable for high temperature load bearing. Pentamolybdenum trisilicide (Mo_5Si_3) has a high

melting point of 2160 °C and a more complex unit cell that may lead to better creep resistance. A major drawback to its application has been the fact that its oxidation resistance is greatly inferior to that of $MoSi_2$. Undoped Mo_5Si_3 exhibits pest oxidation at 800 °C. Mass loss occurs in the temperature range of 900 to 1200 °C due to volatilization of molybdenum oxide, indicating that the silica scale that forms does not provide a passivating layer.

Recently it has been shown that small additions of boron to Mo_5Si_3 significantly improve oxidation resistance (Ref 114). The addition of boron results in protective scale formation and parabolic oxidation kinetics in the temperature range of 1050 to 1300 °C. The oxidation rate of Mo_5Si_3 is decreased by five orders of magnitude at 1200 °C by doping with less than 2 wt% boron. Boron doping eliminates catastrophic pest oxidation at 800 °C. The mechanism for improved oxidation resistance of boron-doped Mo_5Si_3 is viscous sintering of the scale to close pores that form during the initial transient oxidation period due to volatilization of molybdenum oxide. Additionally, the boron forms a multiphase composite material consisting in $Mo_5Si_3B_x$, $Mo_5(SiB)_3$, Mo_3Si, $MoSi_2$, and MoB, with the exact phase composition depending on the level of boron addition. Boron-Mo_5Si_3 materials have been reported to possess good elevated temperature creep resistance.

10. Conclusions

The following conclusions have been drawn in this article:

- Molybdenum disilicide ($MoSi_2$) and its composites have become an important class of high temperature structural materials. They are borderline ceramic-intermetallic compounds, and thus both metal and ceramic processing techniques are very important in developing these silicide based materials. $MoSi_2$ composites are important elevated temperature structural materials for applications in oxidizing and aggressive environments.
- Molybdenum disilicide-based heating elements have been used extensively in high-temperature furnaces. The low electrical resistance of silicides in combination with higher thermal stability, electron-migration resistance, and excellent diffusion-barrier characteristics are important for microelectronic applications.
- Current potential applications of $MoSi_2$-based materials also include combustion chamber parts, missile nozzles, molten metal lances, industrial gas burners, diesel engine glow plugs, and materials for glass processing. Much interest and effort have been invested in the research and development of $MoSi_2$-based materials, and they are expected to enter other applications soon. Improvements in low temperature fracture toughness and high temperature creep resistance are still the most challenging tasks.

References

1. F.O. Soechting, A Design Perspective on Thermal Barrier Coatings, *Thermal Barrier Coating Workshop–Proceedings of a Conference at NASA Lewis Research Center* (Cleveland, OH) 27-29 March 1995, NASA Conference Publication 3312, p 1-15
2. A.K. Vasudevan and J.J. Petrovic, A Comparative Overview of Molybdenum Disilicide Composites, *Mat. Sci. Eng. A*, Vol 155, 1992, p 1-17
3. J.J. Petrovic, High Temperature Structural Silicides, *Ceram. Eng. Sci. Proc.*, Vol 18, 1997, p 3-17
4. J.J. Petrovic and A.K. Vasudevan, Overview of High Temperature Structural Silicides, *Mat. Res. Soc. Symp. Proc.*, Vol 322, 1994, p 3-8
5. J.J. Petrovic, $MoSi_2$-Based High Temperature Structural Silicides, *MRS Bulletin, XVIII*, 1993, p 35-40
6. K.S. Kumar and C.T. Liu, Ordered Intermetallic Alloys, Part II: Silicides, Trialuminides, and Others, *JOM*, June 1993, p 28-34
7. O. Hoenigsschmid, *Monatsh. Chem.*, Vol 28, 1907, p 1017
8. Kanthal, Swedish Patent 155,836, 1953
9. E.A. Brandes and G.B. Brook, *Smithells Metals Reference Book*, 7th ed., 1992, p 11-376
10. W.J. Boettinger, J.H. Perepezko, and P.S. Frankwicz, Application of Ternary Diagrams to the Development of $MoSi_2$-Based Materials, *Mater. Sci. Eng. A*, Vol 155, 1992, p 33-44
11. B.K. Yen, T. Aizawa, and J. Kihara, Influence of Powder Composition and Milling Media on the Formation of Molybdenum Disilicide by a Mechanically Induced Self-Propagating Reaction, *J. Am. Ceram. Soc.*, Vol 79, 1996, p 2221-2223
12. R.B. Schwarz, S.R. Srinivasan, J.J. Petrovic, and C.J. Maggiore, Synthesis of Molybdenum Disilicide by Mechanical Alloying, *Mat. Sci. Eng. A*, Vol 155, 1992, p 75-84
13. S. Zhang and Z.A. Munir, Synthesis of Molybdenum Disilicides by the Self-Propagating Combustion Method, *J. Mater. Sci.*, Vol 26, 1991, p 3685-3688
14. S.C. Deevi, Self-Propagating High-Temperature Synthesis of Molybdenum Disilicide, *J. Mater. Sci.*, Vol 26, 1991, p 3343-3353
15. S.N. Patankar, S.-Q. Xiao, J.J. Lewandowski, and A.H. Heuer, The Mechanism of Mechanical Alloying of $MoSi_2$, *J. Mater. Res.*, Vol 8, 1993, p 1311-1316
16. P.-Y. Lee, T.-R. Chen, J.-L. Yang, and T.S. Chin, Synthesis of $MoSi_2$ Powder by Mechanical Alloying, *Mater. Sci. Eng. A*, Vol 192/193, 1995, p 556-562
17. L. Liu, F. Padella, W. Guo, and M. Magini, Solid State Reactions Induced by Mechanical Alloying in Metal-Silicon Systems, *Acta Metall. Mater.*, Vol 43, 1995, p 3755-3761
18. M.S. Haji-Mahmood and L.S. Chumbley, Processing and Characterization of Nanocrystalline Molybdenum Disilicide Consolidated by Hot Isostatic Pressing (HIP), *Nanostructured Mater.*, Vol 7, 1996, p 95-112
19. T.J. Trentler, R. Suryanarayanan, S.M.L. Sastry, and W.E. Buhro, Sonochemical Synthesis of Nanocrystalline Molybdenum Disilicide ($MoSi_2$), *Mater. Sci. Eng. A*, Vol 204, 1995, p 193-196
20. E. Gaffet and N. Malhhouroux-Gaffet, Nanocrystalline $MoSi_2$ Phase Formation Induced by Mechanically Activated Annealing, *J. Alloy. Compd.*, Vol 205, 1994, p 27-34
21. R. Radhakrishnan, S. Bhaduri, and C.H. Henager, Jr., The Reactive Processing of Silicides, *JOM*, Jan 1997, p 41-45
22. A.K. Bhattacharya, *J. Am. Ceram. Soc.*, Vol 74, 1991, p 2707
23. J. Trambukis and Z.A. Munir, *J. Am. Ceram. Soc.*, Vol 73, 1990, p 1240
24. S.B. Bhaduri, R. Radhakrishnan, and Z.B. Qian, *Scr. Met. Mater.*, Vol 29, 1993, p 1089
25. S.C. Deevi, *Mater. Sci. Eng. A*, Vol 149, 1992, p 241
26. S.C. Deevi, *J. Mater. Sci.*, Vol 26, 1991, p 3343
27. S. Zhang and Z.A. Munir, *J. Mater. Sci.*, Vol 26, 1991, p 3685
28. I.J. Shon, Z.A. Munir, K. Yamazaki, and K. Shoda, Simultaneous Synthesis and Densification of $MoSi_2$ by Field-Activated Combustion, *J. Am. Ceram. Soc.*, Vol 79, 1996, p 1875-1880
29. N.N. Thadhani, *J. Appl. Phys.*, Vol 76, 1994, p 2129
30. L.H. Yu and M.A. Meyers, *J. Mater. Sci.*, Vol 26, 1991, p 601

31. H.O. Pierson, *Handbook of Chemical Vapor Deposition,* Noyes Publications, NJ, 1992
32. W.B. Hillig and M. Usta, Formation Kinetics of $MoSi_2$ and Mo_5Si_3 by the Reactive Diffusive Siliciding of Molybdenum, *J. Am. Ceram. Soc.,* Vol 80, 1997, p 1723-1726
33. A. Makris, Function of Cermet Elements in Heat Treating Furnaces, *Ind. Heat.,* November 1994, p 46-50
34. R.K. Wade and J.J. Petrovic, Fracture Modes in $MoSi_2$, *J. Am. Ceram. Soc.,* Vol 75, 1992, p 1682-1684
35. R.K. Wade and J.J. Petrovic, Processing Temperature Effects on Molybdenum Disilicide, *J. Am. Ceram. Soc.,* Vol 75, 1992, p 3160-3162
36. S.M.L. Sastry, R. Suryanarayanan, and K.L. Jerina, Consolidation and Mechanical Properties of $MoSi_2$-Based Materials, *Mater. Sci. Eng. A,* Vol 192/193, 1995, p 881-890
37. R. Suryanarayanan, S.M.L. Sastry, and K.L. Jerina, Strength and Toughness of Silicide Matrix Materials Consolidated by Hot Isostatic Pressing, *Mat. Res. Soc. Symp. Proc.,* Vol 322, 1994, p 191-196
38. R. Suryanarayanan, S.M.L. Sastry, and K.L. Jerina, Consolidation of Molybdenum Disilicide Based Materials by Hot Isostatic Pressing (HIP): Comparison with Models, *Acta Metall. Mater.,* Vol 42, 1994, p 3741-3750
39. R. Suryanarayanan, S.M.L. Sastry, and K.L. Jerina, Mechanical Properties of Molybdenum Disilicide Based Materials Consolidated by Hot Isostatic Pressing (HIP), *Acta Metall. Mater.,* Vol 42, 1994, p 3751-3755
40. R. Suryanarayanan, S.M.L. Sastry, and K.L. Jerina, On the Values of Material Property Data Used in Hot Isostatic Pressing Models, *Scri. Metall. Mater.,* Vol 28, 1993, p 797-802
41. R. Tiwari, H. Herman and S. Sampath, Vacuum Plasma Spraying of $MoSi_2$ and Its Composites, *Mater. Sci. Eng. A,* Vol 155, 1992, p 95-100
42. R.G. Castro, R.W. Smith, A.D. Rollett, and P.W. Stanek, Ductile Phase Toughening of Molybdenum Disilicide by Low Pressure Plasma Spraying, *Mater. Sci. Eng. A,* Vol 155, 1992, p 101-108
43. T.A. Lograsso, Synthesis of $MoSi_2$ Single Crystals, *Mater. Sci. Eng. A,* Vol 155, 1992, p 115-120
44. O. Thomas, J.P. Senateur, R. Madar, O. Laboide, and E. Rosencher, *Solid State Commun.,* Vol 55, 1985, p 629
45. Y. Umakoshi, T. Hirano, T. Sakagami, and T. Yamane, *Scr. Metall.,* Vol 23, 1989 p 159
46. K. Kimura, M. Nakamura, and T. Hirano, *J. Mater. Sci.,* Vol 25, 1990, p 2487
47. F.A. Cotton and G. Wilkinson, *Advanced Inorganic Chemistry,* 5th ed., Wiley, 1988 p 278-279
48. S.A. Maloy, J.J. Lewandowski, A.H. Heuer, and J.J. Petrovic, Effects of Carbon Additions on the High Temperature Mechanical Properties of Molybdenum Disilicide, *Mater. Sci. Eng. A,* Vol 155, 1992, p 159-163
49. U. Ramamurty, S. Suresh, and J.J. Petrovic, Effect of Carbon Addition on Elevated Temperature Crack Growth Resistance in (Mo, W)Si_2-SiC_p Composite, *J. Am. Ceram. Soc.,* Vol 77, 1994, p 2681-2688
50. N.S. Jacobson and K.N. Lee, Chemical Reactions in the Processing of $MoSi_2$ + Carbon Compacts, *J. Am. Ceram. Soc.,* Vol 76, 1993, p 2005-2009
51. J. Schlichting, Molybdenum Disilicide as a Component of Modern High Temperature Composites, *High Temp.—High Press.,* Vol 10, 1978, p 241
52. E. Fitzer and W. Remmele, Possibilities and Limits of Metal Reinforced Refractory Silicides Especially Molybdenum Disilicide, *Proc. Fifth Int. Conf. on Composite Materials, ICCM-V,* W.C. Harrigan, Jr., J. Strife, and A.K. Dhingra, Ed., AIME, Warrendale, PA, 1985, p 515
53. F.D. Gac and J.J. Petrovic, *J. Am. Ceram. Soc.,* Vol 68, 1985, p C200
54. D.H. Carter, W.S. Gibbs, and J.J. Petrovic, Mechanical Characterization of SiC Whisker-Reinforced $MoSi_2$, *Proc. Third Int. Symp. on Ceramic Materials and Components for Engines,* American Ceramic Society, 1989, p 977
55. L. Xiao and R. Abbaschian, Interfacial Modification in Nb/$MoSi_2$ Composites and Its Effects on Fracture Toughness, *Mater. Sci. Eng. A,* Vol 155, 1992, p 135-146
56. L. Shaw and R. Abbaschian, Control of the Interfacial Reactions in Nb-Toughened $MoSi_2$, *J. Am. Ceram. Soc.,* Vol 76, 1993, p 2305-2311, 1993
57. R. Gibala, A.K. Ghosh, D.C. Van Aken, D.J. Srolovita, A. Basu, H. Chang, D.P. Mason, and W. Yang, Mechanical Behavior and Interface Design of $MoSi_2$-Based Alloys and Composites, *Mater. Sci. Eng. A,* Vol 155, 1992, p 147-158
58. D.E. Alman, K.G. Shaw, N.S. Stoloff, and K. Rajan, Fabrication, Structure and Properties of $MoSi_2$-Base Composites, *Mater. Sci. Eng. A,* Vol 155, 1992, p 85-94
59. M.J. Maloney and R.J. Hecht, Development of Continuous-Fiber-Reinforced $MoSi_2$-Base Composites, *Mater. Sci. Eng. A,* Vol 155, 1992, p 19-32
60. S.K. Ramaseshan and K. Shobu, Reactive Infiltration of Aluminum into Molybdenum Disilicide Preform, *J. Am. Ceram. Soc.,* Vol 81, 1998, p 730-732
61. A. Costa e Silva and M.J. Kaufman, Microstructural Modification of $MoSi_2$ through Aluminum Additions, *Scr. Metall. Mater.,* Vol 29, 1993, p 1141-1145
62. D.H. Carter, W.S. Gibbs, and J.J. Petrovic, Mechanical Characterization of SiC Whisker-Reinforced $MoSi_2$, *Proc. Third Int. Symp. on Ceramic Materials and Components for Engines,* American Ceramic Society, 1989, p 977
63. J.I. Lee, N.L. Hecht, and T-I. Mah, In Situ Processing and Properties of SiC/$MoSi_2$ Nano-Composites, *J. Am. Ceram. Soc.,* Vol 81, 1998, p 421-424
64. J-M. Ting, Sintering of Silicon Carbide/Molybdenum Disilicide Composites Using Boron Oxide as an Additive, *J. Am. Ceram. Soc.,* Vol 77, 1994, p 2751-2752
65. C.H. Henager, Jr., L.J. Brimhall, and J.P. Hirth, *Synthesis of a $MoSi_2$-SiC Composite in situ Using a Solid State Displacement Reaction,* 1992, p 109-114
66. D.E. Lawrynowicz, J. Wolfenstine, B. Hillig, and M. Usta, Reactive Synthesis and Characterization of $MoSi_2$/SiC Using Low Pressure Plasma Deposition and 100% Methane, *J. Am. Ceram. Soc.,* Vol 80, 1997, p 1723-1726
67. D.P. Butt, S.A. Maloy, H.H. Kung, D.A. Korzekwa, and J.J. Petrovic, Creep Behavior of $MoSi_2$-SiC Composites, *J. Mater. Res.,* Vol 11, 1996, p 1-9
68. D.P. Butt, D.A. Korzekwa, S.A. Maloy, H.H. Kung, and J.J. Petrovic, Impression Creep Behavior of SiC Particle-$MoSi_2$ Composites, *Mater. Res. Soc. Symp. Proc.,* Vol 322, 1994, p 197-202
69. A.K. Bhattacharya and J.J. Petrovic, Hardness and Fracture Toughness of SiC-Particle-Reinforced $MoSi_2$ Composite, *J. Am. Ceram. Soc.,* Vol 74, 1994, p 2700-2703
70. J.J. Petrovic, A.K. Bhattacharya, R.E. Honnell, T.E. Mitchell, R.K. Wade, and K.J. McClellan, ZrO_2 and ZrO_2-SiC Particle Reinforced $MoSi_2$ Matrix Composites, *Mater. Sci. Eng. A,* Vol 155, 1992, p 259-266
71. J.J. Petrovic, Mechanical Behavior of $MoSi_2$ and $MoSi_2$ Composites, *Mater. Sci. Eng. A,* Vol 192/193, 1995, p 31-37
72. D.E. Lawrynowicz, J. Wolfenstine, E.J. Lavernia, S.R. Nutt, D.E. Bailey, A. Sickinger, and A.M. Hirt, Reactive Synthesis and Characterization of $MoSi_2$/SiC Using Low-Pressure Plasma Deposition and 100% Methane, *Scr. Metall. Mater.,* Vol 32, 1995, p 689-693
73. J.M. Brupbacher, L. Christodoulou, and D.C. Nagle, U.S. Patent 4,710,348, 1987

74. L. Christodoulou, D.C. Nagle, and J.M. Brupbacher, U.S. Patent 4,774,052, 1988
75. D.C. Nagle, J.M. Brupbacher, and L. Christodoulou, U.S. Patent 4,916,029, 1990
76. R.M. Aikin, Jr., Strengthening of Discontinuously Reinforced $MoSi_2$ Composites at High Temperatures, *Mater. Sci. Eng. A*, Vol 155, 1992, p 121-134
77. C.H. Henager and J.L. Brimhall, Synthesis of a $MoSi_2$/SiC Composites In Situ Using a Solid State Displacement Reaction between Mo_2C and Si, *Scr. Metall. Mater.*, Vol 26, 1992, p 585-589
78. C.C. Yu, V. Jagasivamani, R. Kumar, and T.S. Sudarshan, Novel Synthesis of $MoSi_2$ and $MoSi_2$-Al_2O_3 Ultrafine Powders, *Mater. Sci. Technol.*, Vol 13, 1997, p 887-892
79. J.J. Petrovic, M.I. Pena, I.E. Reimanis, M.S. Sandlin, S.D. Conzone, H.H. Kung, and D.P. Butt, Mechanical Behavior of $MoSi_2$ Reinforced-Si_3N_4 Matrix Composites, *J. Am. Ceram. Soc.*, Vol 80, 1997, p 3070-3076
80. J.J. Petrovic, M.I. Pena, and H.H. Kung, Fabrication and Microstructures of $MoSi_2$ Reinforced-Si_3N_4 Matrix Composites, *J. Am. Ceram. Soc.*, Vol 80, 1997, p 1111-1116
81. H. Klemm, K. Tangermann, C. Schubert, and W. Hermel, Influence of Molybdenum Silicide Additions on High-Temperature Oxidation Resistance of Silicon Nitride Materials, *J. Am. Ceram. Soc.*, Vol 79, 1996, p 2429-2435
82. J.A. Hawk, D.E. Alman, and J.J. Petrovic, Abrasive Wear Behavior of a Si_3N_4-$MoSi_2$ Composite, *J. Am. Ceram. Soc.*, Vol 79, 1996, p 1297-1302
83. K. Arata, N. Takeuchi, M. Yoshinaka, K. Hirota, and O. Yamaguchi, Fabrication and Mechanical Properties of Continuously Graded $MoSi_2$-ZrO_2(2Y) Materials Using Wet-Molding, *J. Am. Ceram. Soc.*, Vol 80, 1997, p 2168-2170
84. R. Gibala, A.K. Ghosh, D.C. Van Aiken, D.J. Srolovitz, A. Basu, H. Chang, D.P. Mason, and W. Yang, Mechanical Behavior and Interface Design of $MoSi_2$-Based Alloys and Composites, *Mater. Sci. Eng. A*, Vol 155, 1992, p 147-158
85. C.M. Huang, C.Y. Yuh, M. Farooque, D. Zhu, Y. Xu, and W.M. Kriven, Properties and Microstructure of Molybdenum Disilicide-β′-$SiAlO_n$ Particle Ceramic Composites, *J. Am. Ceram. Soc.*, Vol 80, 1997, p 2837-2843
86. L.O. Nordberg and T. Ekstrom, Hot-Pressed $MoSi_2$-Particulate-Reinforced α-SiAlON Composites, *J. Am. Ceram. Soc.*, Vol 78, 1995, p 797-800
87. T.C. Chou and T.G. Nieh, Pesting of the High-Temperature Intermetallic $MoSi_2$, *JOM*, December 1993, p 15-22
88. T.C. Chou and T.G. Nieh, *J. Mater. Res.*, Vol 8, 1993, p 214
89. T.C. Chou and T.G. Nieh, *Mater. Res. Proceed.*, Vol 288, 1993, p 965
90. T.C. Chou and T.G. Nieh, *Scr. Metall. Mater.*, Vol 26, 1992, p 1637
91. T.C. Chou and T.G. Nieh, *Scr. Metall. Mater.*, Vol 27, 1992, p 19
92. P.J. Meschter, *Metall. Trans. A*, Vol 23, 1992, p 1763
93. D.A. Berztiss, R.R. Cerchiara, E.A. Gulbransen, F.S. Pettit, and G.H. Meier, *Oxidation of $MoSi_2$ and Comparison with Other Silicide Materials*, 1992, p 165-182
94. J. Cook, A. Khan, E. Lee, and R. Mahapatra, *Oxidation of $MoSi_2$-Based Composites*, 1992, p 183-198
95. A. Mueller, G. Wang, R.A. Rapp, E.L. Courtright, and T.A. Kircher, *Oxidation Behavior of Tungsten and Germanium-Alloyed Molybdenum Disilicide Coatings*, 1992, p 199-208
96. M.K. Meyer and M. Akinc, Isothermal Oxidation Behavior of Mo-Si-B Intermetallics at 1450 °C, *J. Am. Ceram. Soc.*, Vol 79, 1996, p 2763-2766
97. P.H. Boldt, J.D. Embury, and G.C. Weatherly, *Room Temperature Microindentation of Single Crystal $MoSi_2$*, 1992, p 251-258
98. K. Ito, H. Inui, Y. Shirai, and M. Yamaguchi, Plastic Deformation of $MoSi_2$ Single Crystals, *Philos. Mag. A*, Vol 72, 1995, p 1075-1097
99. L. Xiao, Y.S. Kim, and R. Abbaschian, *Mater. Sci. Eng. A*, Vol 144, 1991, p 277-285
100. H.E. Deve, C.H. Weber, and M. Maloney, *Mater. Sci. Eng. A*, Vol 153, 1992, p 668-675
101. S. Maloy, A.H. Heuer, J.J. Lewandowski, and J.J. Petrovic, *J. Am. Ceram. Soc.*, Vol 74, 1991, p 2704
102. K.K. Richardson and D.W. Freitag, *Ceram. Eng. Sci. Proc.*, Vol 12, 1991, p 1679
103. J.J. Petrovic, R.E. Honnell, T.E. Mitchell, T.E. Wade, and K.J. McClellan, *Ceram. Eng. Sci. Proc.*, Vol 12, 1991, p 1633
104. K. Sadananda, H. Jones, J. Feng, J.J. Petrovic, and A.K. Vasudevan, *Ceram. Eng. Sci. Proc.*, Vol 12, 1991, p 1671
105. S. Bose, Engineering Aspect of Creep Deformation of Molybdenum Disilicide, *Mater. Sci. Eng. A*, Vol 155, 1992, p 217-226
106. S.M. Wiederhorn, R.J. Gettings, D.E. Roberts, C. Ostertag, and J.J. Petrovic, Tensile Creep of Silicide Composites, *Mater. Sci. Eng. A*, Vol 155, 1992, p 1-17, 209-216
107. K. Sadananda, C.R. Feng, H. Jones, and J.J. Petrovic, Creep of Molybdenum Disilicide Composites, *Mater. Sci. Eng. A*, Vol 155, 1992, p 227-240
108. W.-Y. Lin, J-Y. Hsu, and R.F. Speyer, Stability of Molybdenum Disilicide in Combustion Gas Environments, *J. Am. Ceram. Soc.*, Vol 77, 1994, p 1162-1168
109. R.G. Castro, J.R. Hellmann, A.E. Segall, and D.L. Shellman, Fabrication and Testing of Plasma-Spray Formed $MoSi_2$ and $MoSi_2$ Composite Tubes, *Mater. Res. Soc. Symp. Proc.*, Vol 322, 1994, p 81-86
110. A.H. Bartlett, R.G. Castro, D.P. Butt, H. Kung, and J.J. Petrovic, Plasma Sprayed $MoSi_2$/Al_2O_3 Laminate Composite Tubes as Lances in Pyrometallurgical Operations, *Ind. Heat.*, Jan 1996
111. S.K. Sundaram and R.F. Speyer, Electrochemical Corrosion and Protection of Molybdenum and Molybdenum Disilicide in a Molten Soda-Lime Silicate Glass Environment, *J. Am. Ceram. Soc.*, Vol 79, 1996, p 1851-1856
112. S.K. Sundaram, J-Y. Hsu, and R.F. Speyer, Molten Glass Corrosion Resistance of Immersed Combustion-Heating Tube Materials in E-Glass, *J. Am. Ceram. Soc.*, Vol 78, 1995, p 1940-1996
113. S.K. Sundaram, J-Y. Hsu, and R.F. Speyer, Molten Glass Corrosion Resistance of Immersed Combustion-Heating Tube Materials in Soda-Lime-Silicate Glass, *J. Am. Ceram. Soc.*, Vol 77, 1994, p 1613-1623
114. M.K. Meyer and M. Akinc, Oxidation Behavior of Boron-Modified Mo_5Si_3 at 800-1300 °C, *J. Am. Ceram. Soc.*, Vol 79, 1996, p 938-944